



Oxygen reduction in alkaline solution at glassy carbon surfaces and the role of adsorbed intermediates



Haozhi Zhang, Chuhong Lin, Lior Sepunaru, Christopher Batchelor-McAuley, Richard G. Compton*

Department of Chemistry, Physical and Theoretical Chemistry Laboratory, University of Oxford, South Parks Road, Oxford OX1 3QZ, United Kingdom

ARTICLE INFO

Keywords:

Electrochemistry
Oxygen reduction
Electron transfer kinetics
Carbon surfaces
Adsorbed intermediates

ABSTRACT

Oxygen reduction at glassy carbon (GC) exhibits distinctively different voltammetric behavior at high (> 10) and low (< 10) pH. The peak potential is found to be around -0.4 V at pH 13, compared to -0.6 V at pH 7.4 as measured against a saturated calomel reference electrode. Using experimental voltammetry and numerical simulation, the difference in peak potential is interpreted in terms of a difference in reaction mechanism. At low pH, O_2 reduction is evidenced to proceed via a solution phase pathway initially resulting in the reduction of oxygen to superoxide. Conversely, at higher pH, a different mechanism is favored involving the formation of a surface bound superoxide species. The switch between the two mechanisms is related to the protonation of the surface bound intermediate under less basic conditions.

1. Introduction

The voltammetric reduction of oxygen on a glassy carbon electrode is unusual in that the reduction is found to occur at a lower potential under more alkaline conditions [1–3]. For example at pH 13 the peak potential is ca. -0.40 V, whereas at pH 7.4 it is ca. -0.60 V. This anodic shift in the position of the voltammetric wave is the opposite of that predicted thermodynamically on the basis of the Nernst equation. Due to the occurrence of coupled protonation steps during the course of the reduction the reaction is overall less energetically favorable at higher pH [4,5]. Consequently, if the reduction were reversible, the peak potential – in contrast to experiment – would be predicted to occur at a more cathodic (negative) potential under alkaline conditions. This unusual voltammetric behavior was recognized and reported as early as the 1970s by Taylor and Humphray [1,2]; however, it took until the 1990s and the work of McCreery [6,7] for the physical origin of this altered behavior to be illuminated.

The oxygen reduction reaction involves the transfer of multiple electrons and protons. At catalytic materials such as platinum, oxygen reduction may result in the production of water via a four electron reduction process [10]. However, at carbonaceous materials the reduction process at potentials less than -1 V (vs SCE) proceed no further than the two-electron reduction to the associated peroxide species [11–13].

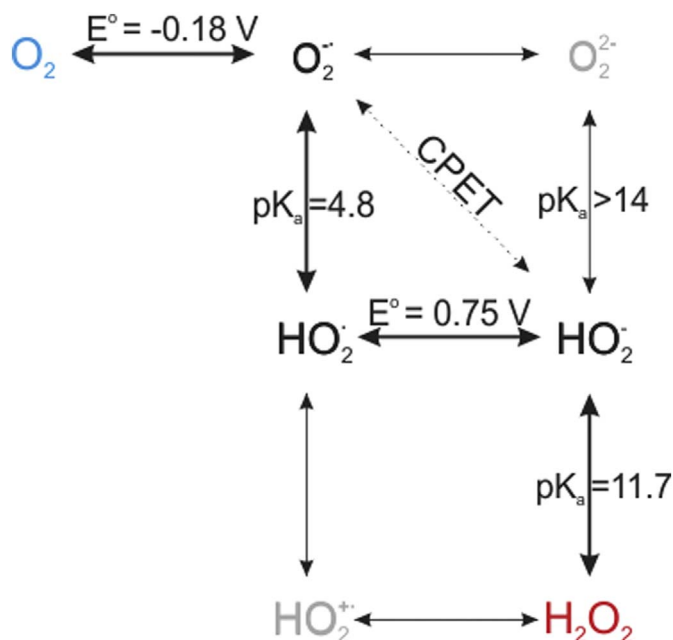
If adsorption processes are absent, the elementary steps of this two-electron two-proton redox process can be summarized using a ‘scheme-

of-squares’, [14–16] as shown in Scheme 1. In this diagram a horizontal movement corresponds to an electron transfer and a vertical shift relates to a proton transfer, a concerted proton-electron transfer process [17] may be represented by a diagonal, as for example indicated by the dashed line in Scheme 1. The exact mechanistic pathway taken will depend on a diversity of factors including the local solution pH, the electrode potential, the formal potentials of the one-electron redox processes, the pK_a of the associated intermediates and the kinetics of each fundamental step. In the case of oxygen the scheme is somewhat simplified since a number of the intermediates likely do not exist in the solution phase. In particular the peroxide species HO_2^- likely has a pK_a significantly outside of the aqueous range (i.e. > 14) [8]. At all values of pH the disproportionation of the superoxide intermediate, $O_2^{\cdot-}$, to oxygen and peroxide is highly thermodynamically favorable; however, in alkaline solutions and in the absence of a suitable catalyst superoxide is found to be relatively kinetically stable, with a reported bimolecular reaction rate of $< 0.3 \text{ M}^{-1} \text{ s}^{-1}$ at pH 14 [18].

Given the significance of the oxygen reduction reaction and the common place use of carbonaceous materials as either an electrode support or as catalysts in and of themselves, [19,20] the present work furthers study of the oxygen reduction mechanism at a glassy carbon electrode under neutral and alkaline conditions. Despite the insightful work of Yang and McCreery [6], who briefly mentioned possible causes for this change in voltammetry at low and high pH, the exact mechanistic pathway remains unclear. It is evidenced in this paper that at both pH 7 and 13, the rate determining step for the electro-

* Corresponding author.

E-mail address: Richard.compton@chem.ox.ac.uk (R.G. Compton).



Scheme 1. Scheme-of-squares for the oxygen/hydrogen peroxide redox couple. Note potential are reported taking the standard state for all species as unit activity. Dashed diagonal represents a possible concerted-proton-electron transfer (CPET) process. pK_a values taken from [8] and standard potentials (vs SHE) calculated from data given in [9].

chemical reduction process is the first electron transfer resulting in the formation of the superoxide intermediate. Simulations show the kinetics of the first electron transfer process is significantly faster under the more alkaline conditions, resulting in an increase in the *measured* apparent transfer coefficient. This experimental observation is consistent with the reaction proceeding via a surface adsorbed intermediate at high pH. It is proposed that the strength of the interaction between the electrode surface and the reduction intermediates that enables the electrochemical process to be faster (more ‘electrocatalytic’) under alkaline conditions. A theoretical model accounting for the presence of the adsorbed intermediate is developed, the results of which are in close agreement with the experimental data at high pH. Note that for modelling surface sensitive electrochemical reactions it is important to recognize the presence of the adsorbed intermediate. Due to the finite number of active sites available the behavior of such systems can differ significantly from those in which the intermediates are based in the solution phase [21]. Finally, we seek to build upon these insights and aim to further illuminate the physical origins of the switch in the electrochemical behavior at pH 10, highlighting the likely importance of the electrochemical double layer.

2. Experimental

Chemicals were purchased and used directly without any further purification. These were KOH (Aldrich, 99 + %), H_2O_2 (Fisher, 30%); NaOH (Acros Organics, 98%), $CsOH \cdot H_2O$ (Aldrich, 99 + %), NaCl (BDH ACS 99 + %), KCl (Aldrich 99 + %). Phosphate Buffer (PB) was prepared with 19 mM NaH_2PO_4 (Sigma, 99 + %) and 81 mM Na_2HPO_4 (Sigma, 99%) giving a solution of pH 7.4. All solutions were prepared with deionised water of resistivity not < 18.2 M Ω cm at 298 K (Millipore UHQ, Vivendi, UK) and the pH measured using a Hannah pH 213 meter.

Electrochemical experiments were performed using a three-electrode configuration consisting of a glassy carbon working electrode (GCE, diameter 1.5 mm, CH Instruments, Austin, USA), platinum wire (99.99% GoodFellow, Cambridge, UK) or graphite rod (for hydrogen peroxide reduction, Sigma-Aldrich, Dorset, UK) as counter-electrode, and a saturated calomel electrode (SCE, BAS Inc., Japan) acting as a reference electrode. Voltammetric measurements were recorded using

Autolab PGSTAT20 computer-controlled Potentiostat (EcoChemie, Utrecht, The Netherlands), and the commercial software GPES[®]. The working electrode was polished with 1.0 μ m, 0.3 μ m, and 0.05 μ m aluminium oxide (Buehler Ltd., USA) slurries on a Buehler polishing pad prior to experimentation. The polished electrode was then sonicated in deionised water for 5 min, before placing into an electrochemical cell. Cyclic voltammetry was performed by sweeping the potential linearly from 0 V to -1 V for most experiments, unless stated otherwise. All reported results are referenced against SCE, which is + 0.24 V against SHE [8]. The solution was saturated with nitrogen or oxygen for at least 20 min before the measurement.

The simulations were made using the commercial available software DigiSim[®] [22,23] or MATLAB[®].

3. Theory and simulation

A model for a two one-electron-transfer reaction at a macroelectrode under semi-infinite diffusion of A and involving an adsorbed intermediate B, is developed, where the reaction is described by the following mechanism:



here A, C are solution-phase species, B is the adsorbate on the electrode, and X refers to an unoccupied active site on the electrode surface. Here the mechanism has been simplified such that the adsorption/desorption of the material from the electrode is considered to occur simultaneously with the electron transfer. For an ion-transfer process i.e. the electro-sorption of material to the surface, viewing the process as being concerted may well, in *some* cases, be a reasonable approximation [24]. As the glassy carbon electrode used in this work is large enough to avoid significant edge effects associated with the mass-transport of material to and from the electrode, in this case, linear semi-infinite diffusion is assumed. In the simulation only the concentration variation in the z direction (perpendicular to the electrode surface) is taken into consideration. For the solution-phase species A and C, the variation of the concentration c with the reaction time t can be described by the Fick's Second Law:

$$\frac{\partial c}{\partial t} = D \nabla^2 c = D \frac{\partial^2 c}{\partial z^2} \quad (3)$$

To solve the above diffusion equation, the boundary conditions of the bulk solution ($z \rightarrow \infty$) and the electrode surface ($z = 0$) are applied. In the bulk solution, the concentrations of A and C keep the initial values c_A^* and c_C^* . On the electrode surface, assuming the two one-electron-transfer steps (1) and (2) are both elementary reactions, with the application of the Fick's First Law, the reaction rates for A, B and C can be calculated:

$$-D_A \frac{\partial c_A}{\partial z} \Big|_{z=0} = -k_{red,1} c_{A(z=0)} \Gamma_X + k_{ox,1} (\Gamma_{max} - \Gamma_X) \quad (4)$$

$$\frac{\partial \Gamma_X}{\partial t} = -k_{red,1} c_{A(z=0)} \Gamma_X + k_{ox,1} (\Gamma_{max} - \Gamma_X) + k_{red,2} (\Gamma_{max} - \Gamma_X) - k_{ox,2} c_{C(z=0)} \Gamma_X \quad (5)$$

$$-D_C \frac{\partial c_C}{\partial z} \Big|_{z=0} = k_{red,2} (\Gamma_{max} - \Gamma_X) - k_{ox,2} c_{C(z=0)} \Gamma_X \quad (6)$$

D_A and D_C ($m^2 s^{-1}$) are the diffusion coefficients of A and C. c_A and c_C ($mol m^{-3}$) are the concentrations of A and C. Γ_X ($mol m^{-2}$) is the surface coverages of the available active sites X and Γ_{max} ($mol m^{-2}$) is the surface coverage of all the active sites available. t is the reaction time. $k_{red,1}$ ($m^3 mol^{-1} s^{-1}$) and $k_{ox,1}$ (s^{-1}) are the reductive and oxidative reaction rate constants of the element reaction step (1), respectively. $k_{red,2}$ (s^{-1}) and $k_{ox,2}$ ($m^3 mol^{-1} s^{-1}$) are the reductive

Download English Version:

<https://daneshyari.com/en/article/4907722>

Download Persian Version:

<https://daneshyari.com/article/4907722>

[Daneshyari.com](https://daneshyari.com)